Amino Acids (2011) 40:123–133
DOI 10.1007/s00726-010-0565-8

ORIGINAL ARTICLE

The structural parameters for antimicrobial activity, human epithelial cell cytotoxicity and killing mechanism of synthetic monomer and dimer analogues derived from hBD3 C-terminal region

L. Zhou · S. P. Liu · L. Y. Chen · J. Li · L. B. Ong · L. Guo · T. Wohland · C. C. Tang · R. Lakshminarayanan · J. Mavinahalli · C. Verma · R. W. Beuerman

Received: 17 December 2009 / Accepted: 10 March 2010 / Published online: 17 April 2010

Abstract Understanding the molecular mechanisms of antimicrobial peptide–membrane interactions is crucial in predicting the design of useful synthetic antimicrobial peptide analogues. Defensins are small (3–5 kDa) cysteine-rich cationic proteins which constitute the front line of host innate immunity. In this study, a series of eight 10 AA C-terminal analogues of hBD3 [sequence: RGRKXXRRKK, X = W, F, Y, V, L, I, H, C(Acm); net charge = +7, coded as W2, F2, Y2, V2, L2, I2, H2, and C2] and covalent V2-dimer [$(RGRKVVRR)_2KK$] (18 AA, net charge = +11) were synthesized using solid phase peptide synthesis (SPPS) in Fmoc chemistry. Wild-type hBD3 was used as a control in all analyses. W2, V2, and especially Y2 showed high activity selectively against Gram-negative bacteria *Pseudomonas aeruginosa* in the concentration range of 4.3–9.7 μM. The covalent dimeric form of V2-monomer, V2-dimer, showed increased antibacterial killing compared to the monomeric form, V2-monomer. Cytotoxicity assays on a human conjunctival epithelial cell line (IOBA-NHC cells) showed that no change in viable cell number 24 h after constant exposure to all the eight peptide analogues even at concentrations up to 200 μg/ml. Fluorescence correlation spectroscopy (FCS) was used to study the interaction of these peptides against POPC vesicles (neutral; mammalian cell membrane mimic) and POPG vesicles (negatively charged; bacterial cell membrane mimic). Using FCS, significant aggregation and some leakage of Rhodamine dye were observed with POPG with Y2, W2 and V2 at the concentration of 5–10 μM and no significant aggregation or disruption of vesicles was observed for all peptide analogues tested against POPC. V2-dimer induced more leakage and aggregation than the monomeric form. Overall, V2-dimer is the most effective antimicrobial peptide, with aggregation of POPG vesicles observed at concentrations as low as 1 μM. The concentration of 5–10 μM for Y2 from FCS correlated with the concentration of 5 μM (6.25 μg/ml), at which Y2 showed a cooperative increase in the activity. This suggests a structural transition of Y2 in the 2.5–5 μM concentration range resulting in the correlated increased antimicrobial activity. These results and the FCS together with previous NMR and molecular dynamics (MD) suggested that the charge density-based binding affinity, stable covalent dimerization, the ability to dimerize or even oligomerize and adopt a well-defined structure are important physicochemical properties distinguishing more effective cationic antimicrobial peptides.

L. Zhou and S.P. Liu contributed equally to the work.

L. Zhou · S. P. Liu · L. Y. Chen · J. Li · R. Lakshminarayanan · R. W. Beuerman (✉)
Singapore Eye Research Institute, Singapore, Singapore
e-mail: rwbeuer@mac.com

L. Zhou · J. Li · R. W. Beuerman
Department of Ophthalmology,
Yong Loo Lin School of Medicine,
National University of Singapore, Singapore, Singapore

L. B. Ong · L. Guo · T. Wohland
Department of Chemistry,
National University of Singapore, Singapore, Singapore

C. C. Tang
Department of Pharmaceutical Microbiology,
Singapore General Hospital, Singapore, Singapore

J. Mavinahalli · C. Verma
Bioinformatics Institute (ASTAR), Singapore, Singapore

R. W. Beuerman
Duke-NUS Graduate Medical School,
SRP Neuroscience and Behavioral Disorders,
Singapore, Singapore

Keywords Antimicrobial peptides (AMPs) · Human β-defensin 3 (hBD-3) · Covalent dimerization · Cytotoxicity · Fluorescence correlation spectroscopy (FCS)

Introduction

Defensins are a family of endogenous cationic peptides with a molecular mass of 3–5 kDa usually containing three intra-molecular disulfide bonds (Bevins et al. 1999; Diamond and Bevins 1998; Ganz and Lehrer 1995). Defensins are an important component of the innate immune system which provides an initial antimicrobial barrier for mucosal surfaces such as the surface of the eye, oral tissues, the airways and lungs, and also the skin (Cullor et al. 1990; McDermott et al. 2003; Zhou et al. 2004; Li et al. 2006; Dunsche et al. 2002) Their mode of action involves electrostatic interactions with the membrane, leading to permeability changes or pore formation in bacteria, fungi membrane and viruses' envelopes (Hancock et al. 1995; Boman 1995). The low sequence similarity among members of mammalian β-defensin family, but the highly conserved secondary and tertiary structures as well as similarities of charge density suggests that their antimicrobial activity may depend on the structure and charge distribution rather than their primary sequence (Raj and Dentino 2002). Lacking a distinct hydrophobic core, folding of defensins is mainly stabilized by the presence of three disulfide bonds (Bauer et al. 2001). Studies of peptide analogues of human β-defensin 3 (hBD-3) (Dhople et al. 2006; Kluver et al. 2005, 2006) have pointed to the distribution of the positively charged amino acids and hydrophobic side chains as important parameters of antimicrobial activity while the overall hydrophobicity may correlate with cytotoxicity to mammalian cells.

Our previous work demonstrated that full-length linear analogues of hBD-3 might exhibit significantly more potent antimicrobial activity with reduced cytotoxicity than the native hBD3 (Liu et al. 2008). The decreased cytotoxicity of the linear analogs was suggested to be structurally related to the removal of disulfide bridges, and the flexible structure of the linear forms which seemed to be associated with the loss of secondary structure. ^{1}H NMR spectroscopy and extensive molecular dynamics simulations of 10 AA C-terminal analogues of hBD3 showed that the higher density of positive charges within the scaffold of a well-defined structure might predict higher antimicrobial activity (Bai et al. 2009).

The goal of the present study was to determine the structural parameters for antimicrobial activity, human epithelial cell cytotoxicity and killing mechanism of small cationic peptides and to understand the molecular mechanisms of antimicrobial peptide–membrane interactions. We designed and synthesized a series of 10-residue C-terminal analogues [sequence: RGRKXXRRKK, X = Y, W, V, F, L, I, C(Acm), H] of hBD3 with the same net charge (+7), but different hydrophobicities through the mutation of the two cysteines with different residues [Tyr, Trp, Val, Phe, Leu, Ile, Cys(Acm) and His]. A branched V2-dimer [$(RGRKVVRR)_2$KK] was designed as a covalent dimeric form of V2-monomer, in which one repeating unit (RGRKVVRR) was linked to the main chain of the second Lys, the another repeating unit was linked to the side chain of the same Lys, thus the two repeating units (RGRKVVRR) are linked to the second Lys in parallel. Some of these short analogues, e.g., W2, V2 and Y2, exhibited good antimicrobial properties selectively against Gram-negative bacteria *Pseudomonas aeruginosa*, which is a common pathogen in eye infections, with little toxicity to human cells. V2-dimer showed greater antimicrobial activity compared to the V2-monomer. Results obtained from FCS in this study and NMR and molecular dynamics (MD) (Bai et al. 2009) indicated that stable dimerization of the peptides played an important role in the mechanism of antimicrobial action. Moreover, the charge density-based binding affinity, the ability to aggregate (e.g., dimerize or even oligomerize) and adopt a well-defined structure are suggested to be important physicochemical properties characterizing more effective cationic antimicrobial peptides.

Materials and methods

Solid phase peptide synthesis (SPPS)

Recombinant wild-type hBD3 was purchased from CytoLab Ltd. A series of C-terminal analogues [sequence: RGRKXXRRKK, X = Y, W, V, F, L, I, C(Acm), H, coded as Y2, W2, V2, F2, L2, I2, C2 and H2 of hBD-3] and covalent V2-dimer were prepared using SPPS in Fmoc chemistry. The general protocol for synthesis and purification was reported in our previous work (Liu et al. 2008). For further purification, the crude products were dissolved in a solvent containing 5% ACN and 0.1% TFA in H_2O and loaded onto a semi-preparative HPLC column (Delta PAK C18, 300 × 7.8 mm I.D., 15 μm, 100 Å, Waters Associates, Milford, MA) at a flow rate of 3 ml/min. The Waters HPLC system is equipped with a 2690 separation module, an autosampler and a 996 photodiode array detector (PDA) (Waters Associates, Milford, MA). Gradient elution was started at 98% A/2% B (eluent A, 0.01% TFA in water; eluent B, 0.01% TFA in ACN) and linearly changed to 67% A/33% B in 33 min. The chromatogram was monitored by PDA at 210 nm. The identification of molecular mass of the final

product was confirmed by HPLC–ESI-MS (Micromass Platform LCZ, Manchester, UK) using a Delta PAK C18, 150 × 3.9 mm I.D., 5 μm, 100 Å (Waters Associates, Milford, MA) at a flow rate of 0.2 ml/min. A gradient profile of eluent B (ACN) increasing from 2 to 15.5% in 30 min and then 15.5–31% in 3 min of eluent B was used.

Molecular hydrophobicity analysis

The system of reverse phase (RP)-HPLC–ESI-MS was used to monitor the elution of the peptides by chromatography. The overall molecular hydrophobicity of peptides was characterized in terms of retention time of peptide peak and the corresponding ACN % of the peptide peak. ACN % was calculated from these data of retention time obtained by HPLC–ESI-MS based on the gradient profile. The experiments were conducted under the same conditions, e.g., the column [a Delta PAK C18, 150 × 3.9 mm I.D., 5 μm, 100 Å (Waters Associates, Milford, MA)], the peptide concentration (500 μg/ml), injection volume (5 μl) and flow rate of 0.2 ml/min and the gradient profile [2–15.5% in 30 min and then 15.5–31% in 3 min of eluent B (ACN)]. The relative overall hydrophobicities of these analogues were calculated and determined using the amino acid hydrophilicity scale of Hopp–Woods (1981). The scale of Hopp–Woods was derived for predicting potential antigenic sites of globular proteins, which are likely to be rich in charged and polar residues.

Antimicrobial activity assays

Gram-negative bacteria *P. aeruginosa* ATCC 9027 was used in the study. It was chosen because *P. aeruginosa* is known to cause corneal ulcers that are difficult to treat and often require an intensive regimen of fortified topical antibiotics. Resistance to some commonly used antibiotics has been documented among clinical ocular isolates of *P. aeruginosa*, thus adding to a sense of urgency in the search for alternative therapeutic agents (Parks and Hobden 2005). Bacteria not more than five passages were removed from the original master lot obtained from the American Type Culture Collection (ATCC). Bacteria were prepared with a final cell count of 10^5–10^6 cfu/ml (cfu is colony forming unit). Cfu of surviving bacteria is counted after incubating with test peptides at 22.5°C for 4 h in USP phosphate buffer, pH 7.2. The antibacterial activity of the peptide was manifested as the logarithmic (log) reduction of the bacteria on exposure to the peptide. Bacteria unexposed to peptides were also counted parallel to the test as control.

Cytotoxicity assay

For the cytotoxicity assays, the primary concern was for the fragile epithelial cells that cover the surface of the surface of the eye. The surface of the eye is a mucosal surface and an important use of AMPs would be for the eye or other mucosal surfaces such as the lungs and mouth all of which have an epithelial cell covering (Liu et al. 2008). Cytotoxicity was determined by measuring the amount of ATP generated by viable cells in culture using the CellTiter-Glo luminescent cell viability assay (Promega, Madison, WI). Peptides were incubated with a human conjunctival epithelial cell line (IOBA-NHC) as described previously (Liu et al. 2008; Diebold et al. 2003) The luminescent signal was read by a microplate reader (Tecan GeniosPro, Tecan Asia, Singapore). Blank wells containing only medium were included in each assay and the reading was subtracted from each sample and control well. Using the luminescence of the un-treated wells as 100%, cell viability was calculated as (luminescence of control − luminescence of sample)/luminescence of control × 100%. Each condition was assayed in triplicate, and the experiments were repeated three time.

Fluorescence correlation spectroscopy (FCS)

Materials

1-Palmitoyl-2-Oleoyl-sn-Glycero-3-Phosphocholine (POPC), 1-Palmitoyl-2-Oleoyl-sn-Glycero-3-[Phospho-rac-(1-glycerol)] (POPG), and 1,2–Dipalmitoyl-sn-Glycero-3-Phosphoethanolamine-*N*-(Lissamine Rhodamine B Sulfonyl) (Ammonium Salt) (Rho-PE) were purchased from Avanti (Avanti Polar Lipids, Inc., Alabaster, AL).

Rho 6G entrapping large unilamellar vesicle (REV) preparation

Lipids were prepared as stock solutions in chloroform. The solvent was evaporated under N2 gas and then the samples were placed into vacuum for at least 1 h. Phosphate buffered saline (PBS) (10 mM phosphate buffer containing 138 mM NaCl and 2.7 mM KCl at pH 7.4) including 1 μM Rho 6G was added to prepare a lipid suspension with lipid concentration of 0.5 mM. After 5 freeze–thawing cycles the suspension was extruded through 0.1 μm membranes. MicroSpini S-200 h Columns (Amersham Biosciences, Singapore) were used to remove free Rho 6G from the vesicle solution (Pramanik et al. 2000).

Rho-PE labeled large unilamellar vesicle (RLV) preparation

The preparation of RLVs followed a similar protocol as above. Phospholipid was mixed with 0.1% Rho-PE in a volatile organic solvent. After completely removing the solvent, PBS was added to form a suspension of

phospholipids. RLVs were obtained by freeze–thawing lipid suspension five times followed by extrusion through 0.1 μm polycarbonate membrane filters. Because the percentage of Rho-PE was very low, RLVs can be used to represent the lipid vesicles under investigation (Pramanik et al. 2000).

Confocal imaging

Confocal imaging was performed on a FluoViewTM FV300 system with a HeNe laser (543 nm). The laser beam was reflected by a long pass dichroic mirror (560DCLP, Omega, Brattleboro, VT) and the scanning mirrors, and focused on the samples using a water immersion objective (UPlanApo, 60×, NA1.2, Olympus, Singapore). The emission of Rho6G and Rho-PE was filtered by a 593AF40 emission filter (Semrock, Rochester, NY).

FCS instrumentation

The FCS system is built around the same confocal microscope as described in the preceding paragraph. For FCS measurements the emission light after the confocal pinhole was focused by a lens (Achromat $f = 60$ mm, Linos), separated from the excitation light by an emission filter (593AF40, Semrock) and collected on an active area of an avalanche photodiode (APD) in a single-photon-counting module (SPCM-AQR-14, Pacer Components, Reading, UK). The signal from the APD was processed online by an autocorrelator (Flex02-01D, correlator.com, Bridgewater, NJ) to obtain an experimental autocorrelation function (ACF) curve. Curve fitting was performed using a self-written program in IgorPro (WaveMetrics, Portland, OR).

FCS data fitting

FCS experiments were performed on solution samples and hence the particles can be assumed to be diffusing freely in three dimensions (3D) governed by Brownian motion. For the 3D diffusion processes of a single fluorescent species, such as vesicles or free fluorophore, the ACF, including a triplet state contribution of the fluorophore, can be fitted as follows:

$$G(\tau) = \frac{1}{N}\left[1 + \frac{F_{\text{trip}}}{1 - F_{\text{trip}}}\exp\left(-\frac{\tau}{\tau_{\text{trip}}}\right)\right]\left(1 + \frac{\tau}{\tau_{\text{D}}}\right)^{-1} \left[1 + \left(\frac{\omega}{z}\right)^2 \frac{\tau}{\tau_{\text{D}}}\right]^{-\frac{1}{2}} + G_\infty \quad (1)$$

with the diffusion time of the particle

$$\tau_{\text{D}} = \frac{\omega^2}{4D}, \quad (2)$$

where N is the average number of particles in the confocal observation volume. F_{trip} is the average fraction of particles that reside in the triplet state and τ_{trip} is the triplet state relaxation time. τ_{D} is the diffusion time of the fluorescent particle through the confocal volume, and is related to the diffusion coefficient D (Eq. 2). ω and z are the radial and axial distances of the confocal volume where the excitation intensity has dropped by $1/e^2$ of the maximum value at the center of the observation volume. G_∞ is the convergence value of the ACF for long times with an expected value of 1.

For two-component 3D diffusion processes, such as the vesicle and the free dye, the ACF with triplet state contribution is given by

$$G(\tau) = \frac{1}{N}\frac{F_1 g_1(\tau) + \left(\frac{Q_2}{Q_1}\right)^2 F_2 g_2(\tau)}{\left(F_1 + \left(\frac{Q_2}{Q_1}\right)^2 F_2\right)^2} + G_\infty \quad (3)$$

with

$$g_i(\tau) = \left(1 + \frac{\tau}{\tau_{\text{Di}}}\right)^{-1}\left(1 + \left(\frac{\omega}{z}\right)^2 \frac{\tau}{\tau_{\text{Di}}}\right)^{-\frac{1}{2}} \left[1 + \frac{F_{\text{trip}}}{1 - F_{\text{trip}}}\exp\left(-\frac{\tau}{\tau_{\text{trip}}}\right)\right]. \quad (4)$$

The fluorescence yield Q_i is the product of the extinction coefficient, the quantum yield, and the overall detection efficiency for particle i in the instrument. The coefficient F_i is the mole fraction of species i in the sample. $g_i(\tau)$ is the characteristic function of the underlying process that causes the fluctuations. τ_{Di} refers to the diffusion time of the fluorescent particle i in the confocal volume. The experimental ACFs were fit with either Eq. 1 or 3, depending on the number of components present in the sample, as described previously (Yu et al. 2008).

FCS measurements

Confocal FCS determines concentrations and diffusion coefficients with single molecule sensitivity by monitoring the fluorescence fluctuation created when of fluorescent particles transition through a small observation volume (Magde et al. 1972). It can therefore be used to determine the size and state of labeled and fluorophore entrapping vesicles and micelles (Yu et al. 2006, 2008; Krouglova et al. 2004). Fluorophore entrapping or fluorophore-labeled vesicles are large structures which will diffuse slowly with typical transition times through a confocal observation volume (~500 nm diameter) of tens of milliseconds. In contrast, fluorescent molecules, with a much smaller size, diffuse faster with typical transition

times in the range of 0.1 ms or faster. Therefore, FCS can distinguish between freely moving fluorophores in solution and intact labeled vesicles. In the case of fluorophore entrapping vesicles, membrane permeation by an agent will lead to leakage of the fluorophore and will thus result in larger diffusion coefficients compared to intact vesicles. To distinguish whether membrane permeation or disruption is the cause of leakage, fluorophore-labeled vesicles can be employed in which the membrane itself is fluorescently labeled. Membrane permeation will not change the size of the vesicles and will therefore not change the diffusion coefficient of the sample. However, membrane disruption will lead to the creation of smaller vesicles or vesicle fragments with much faster diffusion coefficients than the parent vesicles. The two vesicle models combined can then give precise knowledge about vesicle aggregation, leakage and membrane permeation or disruption. Experimental procedure followed our previous publication (Yu et al. 2005). Using FCS, a series of six 10 AA analogues and V2-dimer were tested against POPC-RLV (POPC: a neutral; mammalian cell membrane mimic, RLV: Rhodamine-labeled vesicle) and POPG-RLV and POPG-REV (POPG: negatively charged; bacterial cell membrane mimic, REV: Rhodamine-entrapping vesicle).

Results

Synthesis of peptides by SPPS

A series of eight C-terminal analogues of hBD-3, coded as Y2, W2, V2, F2, L2, I2, C2 and H2, were synthesized via the mutation of two cysteine residues with hydrophobic varying residue by SPPS and their molecular masses were confirmed by HPLC–ESI-MS. V2-dimer was also designed as a covalently branched dimeric form of V2-monomer in parallel and was used to examine the effect of dimerization on antimicrobial activity. Table 1 shows the basic physicochemical properties of these analogues. These analogues are a family of structurally unique analogues, they have the same length (10-residue), very similar sequence (only two cysteines being mutated) and the same net charge (+7), but have different molecular hydrophobicity and different charge density due to different ability to dimerize and accrete well-defined structures upon interactions with lipid membranes (Bai et al. 2009), thus these analogues are expected to display different antimicrobial activity. These 10-residue analogues provide a well-defined model to study the effects of charge density and overall hydrophobicity on antimicrobial, hemolytic and cytotoxic activities.

Table 1 The basic physicochemical property of analogues

Variant	Number of residues		Net positive charge
	Total	Hydrophobic (aromatic) residue	
W2	10	2 (2)	7
F2	10	2 (2)	7
Y2	10	2 (2)	7
L2	10	2 (0)	7
I2	10	2 (0)	7
V2	10	2 (0)	7
H2	10	0 (2)	9[a]
C2	10	0 (0)	7
V2-dimer	18	4 (0)	11

[a] Histidine: weakly basic

Molecular hydrophobicity

We have characterized the overall molecular hydrophobicity in terms of retention time of peptide peak and ACN % of peak at the same concentration, e.g., 500 μg/ml and same HPLC profile (Table 2). RP-HPLC is an approach that is commonly employed for comparisons of peptides or amino acid side chains on antibacterial peptides (Raguse et al. 2002; Schmitt et al. 2007; Liu et al. 2008). Since the stationary phase of C18-modified silica is hydrophobic and the mobile phase (water-acetonitrile) is hydrophilic, longer retention time is a measure of greater hydrophobicity. The measured order for the overall molecular hydrophobicity of these analogues was as follows: W2 > F2 > L2 > I2 > Y2 > V2 > C2 > H2. The relative hydrophobicities of the peptides were also calculated based on the Hopp–Woods hydrophilicity scale (Hopp and Wood 1981) (Table 2). The scale is a hydrophilic index where apolar residues have been assigned negative values, and is typically used to identify antigenic regions based on hydrophilic patches. For each peptide, the values corresponding to each residue were summed to give an overall measure. Lower value corresponds to lower hydrophilicity or higher hydrophobicity. The order for relatively overall hydrophobicity of peptides is: W2 > F2 > Y2 > L2 = I2 > V2 > H2. The general trend in computed hydrophobicity of the peptides using this scale matched that of the experimental HPLC retention time data. C2 [C(Acm)2] was excluded as Acm has not been parameterized in the Hopp–Woods scale.

Antibacterial activity

This series of 10 AA C-terminal analogues exhibited varying antibacterial activities against the common human

Table 2 The overall hydrophobicity of peptides in terms of retention time (Rt) in HPLC–MS and ACN % of peak and relatively overall hydrophobicity by calculation

Variant	Retention time (min) (UV peak)	ACN %[a]	Relatively overall hydrophobicity[b]
W2	32.01 ± 0.20	25.90 ± 1.02	14.2
F2	28.40 ± 0.35	14.78 ± 0.16	16
L2	24.33 ± 0.59	12.95 ± 0.27	17.4
I2	22.29 ± 0.46	12.03 ± 0.21	17.4
Y2	21.46 ± 0.58	11.66 ± 0.26	16.4
V2	17.59 ± 0.32	9.92 ± 0.14	18
C2	17.22 ± 0.31	9.75 ± 0.14	n.c.
H2	11.51 ± 0.18	7.18 ± 0.08	20
V2-dimer	27.20 ± 0.67	24.87 ± 1.26[c]	n.c.

[a] For eight 10-residue analogues, HPLC profile: gradient 2–15.5% in 30 min and then 15.5–31% in 3 min of eluent B (ACN)

[b] The overall hydrophobicity was calculated based on the hydrophobicity scale of Hopp–Woods hydrophilicity scale

[c] For V2-dimer, HPLC profile: gradient 3.5–7% in 15 min and then 7–30% in 15 min of eluent B (ACN)

n.c. not calculated, for C2 and V2-dimer, the two data are not available due to Cys(Acm) or sequence extension both at main chain and side chain of the branched lys in V2-dimer, resulting to unnatural linkage

Table 3 Antimicrobial activity against *Pseudomonas aeruginosa* ATCC 9027 (log reduction)

Variant	100 (μg/ml)	50 (μg/ml)	25 (μg/ml)	12.5 (μg/ml)	6.25 (μg/ml)	3.125 (μg/ml)
Y2	NA	3.07	2.39	2.10	2.02	0.33
W2	NA	4.44	2.48	1.46	1.27	0.53
V2	NA	3.21	1.91	1.74	1.46	0.49
V2-dimer	NA	NA	>6.54	>6.54	2.82	0.59
L2	NA	3.00	1.77	1.66	0.40	0.22
I2	NA	2.99	2.20	1.53	0.51	0.02
F2	0.61	0.87	NA	NA	NA	NA
C2	0.57	0.63	NA	NA	NA	NA
H2	0.62	NA	NA	NA	NA	NA

Peptides were incubated with bacteria *Pseudomonas aeruginosa* ATCC 9027 for 4 h at 22.5°C

0.5 log reduction equals to 68% bacteria being killed; 1 log reduction equals to 90% bacteria being killed; 2 log reduction equals to 99% bacteria being killed; 3 log reduction equals to 99.9% bacteria being killed

NA not available, did not test

pathogen, *P. aeruginosa* ATCC 9027. The antibacterial activity results are shown in Tables 3 and 4. The dimeric form, V2-dimer, was more potent than its monomeric form, V2-monomer. Y2, W2 and V2 monomers showed potent antibacterial activity against *P. aeruginosa* compared with the other five 10-residue analogues. Y2 showed high antibacterial activity in the low concentration range compared to the other peptides. A cooperative increase in the activity of Y2 was detected in concentrations from 3.125 to 6.25 μg/ml (2.5–5.0 μM) in the aqueous conditions (Table 3). This suggests a structural transition of Y2 at 5 μM resulting in its abrupt increased activity. In contrast, relatively low antibacterial activity was observed for H2, C2 and F2. In the high concentration range of 50–100 μM, no detectable transitions to a high activity state were observed in the three peptides in aqueous solution.

Cytotoxicity to mammalian cells

It is well established that cationic peptides not only interact with pathogens, but can also be toxic to mammalian cells. Bacterial cell membranes consist of anionic phosphatidylglycerol as a major component, while eukaryotic cell membranes mainly contain zwitterionic phosphatidylcholine and phosphatidylethanolamine which are susceptible to hydrophobic interactions (Yeaman and Yount 2003). It has been proposed that the hemolytic effects of cationic antimicrobial peptides are directly linked to the

Table 4 Antimicrobial activity against *Pseudomonas aeruginosa* ATCC 9027 (log reduction)

Variant	50 (μg/ml)	25 (μg/ml)	12.5 (μg/ml)	6.25 (μg/ml)
Y2	2.54	2.48	2.02	2.00
W2	2.41	1.91	1.19	1.19
V2	4.39	1.75	0.35	NA
L2	1.20	1.18	1.47	0.32
I2	2.00	1.45	1.46	0.70
Wt hBD3	NA	NA	0.34	0.09
Gentamicin	>5.88	>5.88	>5.88	NA

Peptides were incubated with bacteria *Pseudomonas aeruginosa* ATCC 9027 for 2 h at 22.5°C

0.5 log reduction equals to 68% bacteria being killed; 1 log reduction equals to 90% bacteria being killed; 2 log reduction equals to 99% bacteria being killed; 3 log reduction equals to 99.9% bacteria being killed

NA not available, did not test

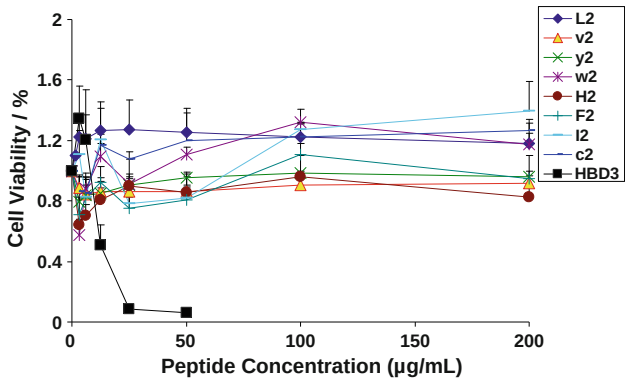

Fig. 1 Cytotoxicity assay of eight 10 AA C-terminal analogues and wt hBD3 for human conjunctival epithelial cells

hydrophobicity of these peptides (Hwang and Vogel 1998). High levels of hydrophobicity are known to decrease selectivity between the desired bacterial target membranes and mammalian host cell membranes. The cytotoxicity of this series of 10 AA C-terminal analogues was tested on a human conjunctival epithelial cell line (IOBA-NHC cells). No obvious decrease in the number of viable human conjunctival epithelial cells was observed 24 h after constant exposure to the eight analogues at concentrations up to 200 μg/ml (Fig. 1). A slight increase of viable cell number was observed in the presence of C2, I2 and W2 in the concentration range of 12.5–200 μg/ml. However, wt hBD-3 at 12.5 μg/ml resulted in around 50% epithelial cell death corroborating an earlier observation (Liu et al. 2008). Only 6% of the cells remained viable after 24 h exposure to hBD-3 at 50 μg/ml. Cytotoxicity showed that this series of analogues are safe even at concentration of 200 μg/ml compared with wt hBD3. The lower hydrophobicity of this series of 10 AA C-terminal analogues is likely to be a primary structural parameter leading to lower toxicity.

Fluorescence correlation spectroscopy

We recorded confocal images of POPG REVs (top), POPG-RLVs (middle), and POPC-RLVs (bottom) in the presence of 1 and 10 μM of six 10-residue analogues and V2-dimer (Fig. 2). For V2-dimer, aggregations of the POPG-RLVs and POPG-REVs were observed with 1 μM V2-dimer; for the six 10-residue analogues, V2, W2, Y2, F2, L2 and I2, no antibacterial action was observed with 1 μM of peptide while aggregations of the POPG-RLVs and POPG-REVs were observed at a peptide concentration of 10 μM of peptides. The confocal images of POPG-REV and POPG-RLV in the presence of 1 and 10 μM of V2-dimer and V2-monomer showed that the covalent dimeric form was more effective than the monomeric form, indicating that stable dimerization of the peptide has an important role in the mechanism of antimicrobial action. Furthermore, all these analogues showed no effect towards POPC-RLVs even at the high peptide concentration of 10 μM (Fig. 2, bottom), indicating the relatively low cytotoxicity of these antimicrobial peptides.

Figure 3 shows the action of Y2 on Rhodamine-entrapping vesicle (REVs), the correlation curve in B is essentially a combination of curves of vesicles in A and dye in C, indicating POPG-REV leak and aggregate in the presence of 10 μM Y2. Aggregation of POPG-REVs was observed starting from a concentration of 5 μM of Y2 peptide, with some leakage of Rhodamine dye from the REVs detected in the solution. With lower concentrations of Y2 peptide, e.g., 1 μM, no aggregation and no leakage were detected. With higher concentrations of Y2 peptide, mainly aggregation of POPG-REVs was observed with some leakage of Rhodamine detected. Figure 4 displayed FCS curves, showing the interaction of Y2 with Rhodamine-labeled vesicle (RLVs), the width of the curves increased in the presence of 5 μM Y2, indicating POPG-RLV aggregation; however, the width of the curves did not increase even in the presence of 30 μM Y2, no effect of Y2 on the POPC-RLVs was detectable at the high concentration of 30 μM. Aggregation of POPG-RLVs was observed starting from around 5 to 10 μM Y2 peptide. With lower concentrations of Y2 peptide, e.g., 1 μM, no aggregation was detected and with higher concentrations of Y2 peptide, mainly aggregation of POPG-RLVs was observed. This concentration range of 5–10 μM observed from FCS correlated with the effective concentration of Y2 for antibacterial activity, e.g., a cooperative increase in the activity of Y2 was detected in concentrations from 3.125 to 6.25 μg/ml (2.5–5.0 μM) (Table 3) The vesicle aggregation is an important indicator for antimicrobial function.

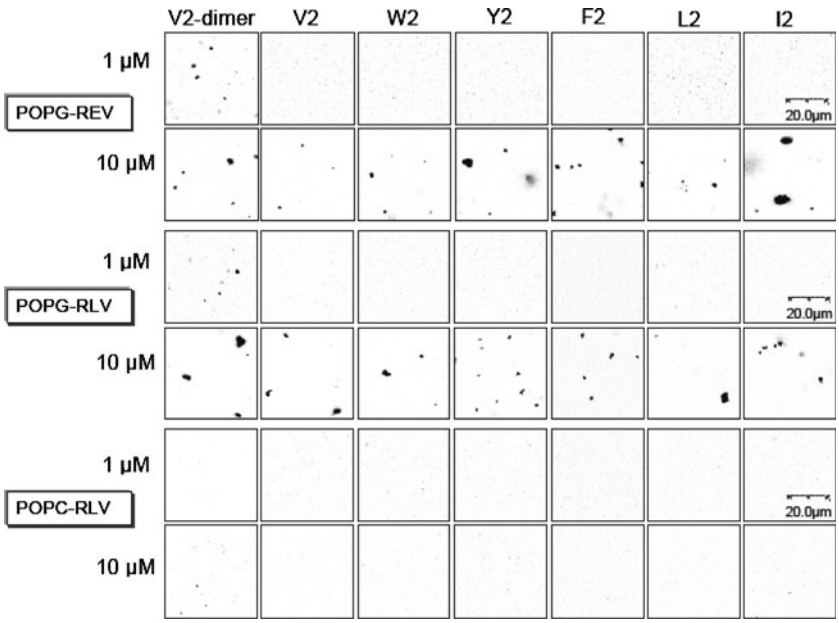

Fig. 2 Confocal image POPG REVs (*top*), POPG-RLVs (*middle*), and POPC-RLVs (*bottom*) in the presence of 1 and 10 μM of antimicrobial peptides

Indeed, the vesicle aggregation studies have been used to infer whether the antimicrobial peptides exert the action by vesicular aggregation or dissociation (Persson et al. 2001). The FCS studies clearly suggest that the designed peptides exert antimicrobial action by aggregations of POPG-REVs and POPG-RLV. The FCS results (e.g., vesicle aggregations were observed for Y2 at 5–10 μM and for V2-dimer at 1 μM) correlate well with antimicrobial activity of peptides [e.g., 2.02, log ~99% for Y2 at 6.25 μg/ml (5 μM) (at this point, noncovalent Y2-dimer is 2.5 μM); 2.82, log ~99.9% for V2-dimer at 6.25 μg/ml (2.74 μM)]. The critical concentration for Y2 and V2-dimer is almost the same [e.g., 6.25 μg/ml (2.5 μM) for noncovalent Y2-dimer and 6.25 μg/ml (2.74 μM) for covalent V2-dimer]. At low concentration (e.g., 3.125 μg/ml), V2-dimer is more potent than Y2, which exists as a monomer (i.e., prior to the structural transition/dimerization).

Discussion

Both antibacterial activity (log reduction) and FCS experiment showed that covalent V2-dimer had greater antibacterial activity against *P. aeruginosa* compared to V2-monomer, indicating stable dimerization of peptides has an important role in the mechanism of antimicrobial action. Our synthetic strategy for the covalent V2-dimer is based on the fact that noncovalent dimerization enhances the antimicrobial activity; therefore, incorporating a branch or covalently connecting the two chains close to the C terminus could reinforce and augment the antimicrobial properties. We designed a branched peptide to obtain a covalently linked stable dimer which we hypothesized would concentrate charge compared to noncovalent Y2-dimer mediated by hydrophobic interactions and π–π stacking of Tyr residues between two Y2-monomers. The noncovalent Y2-dimer is not stable and depends on concentration (Bai et al. 2009). We do not anticipate the covalent V2-dimer structure to be similar to that observed for the noncovalent Y2 dimer by NMR and MD simulations. The origin of cooperative increase in antibacterial activity for V2-dimer in the concentration range of 3.125–6.25 μg/ml (1.37–2.74 μM) could be due to the minimum effective concentration at target site, which is required to kill bacteria. The changes in minimum effective concentration of the antimicrobial peptide at the bacterial membrane for Y2 and V2 are both concentration dependent with differences in effective net charge and charge density. Dimerization/structural transition of Y2 and V2 also contributes to cooperative increase in antibacterial activity. We have also observed that V2-dimer exists as a monomer without dimerization/structural transition in NMR diffusion coefficient measurements even at 500 μM. V2-dimer is more potent than Y2 at the same concentration, it is probably due to a large increase in positively charged residues close to the branch position which, in turn, may increase the charge density. Actually, we have observed that V2-dimer has a compact 3D structure with concentrated charge compared with V2-monomer and Y2 monomer, NMR structure comparison between V2-dimer and V2-monomer gave strong evidence to support this concept.

It was observed that Y2 had a cooperative increase in the antibacterial activity in concentrations from 3.125 to 6.25 μg/ml (2.5–5.0 μM) in the aqueous conditions, this suggests a structural transition of Y2 at 5 μM resulting in its remarkably increased activity. This effective

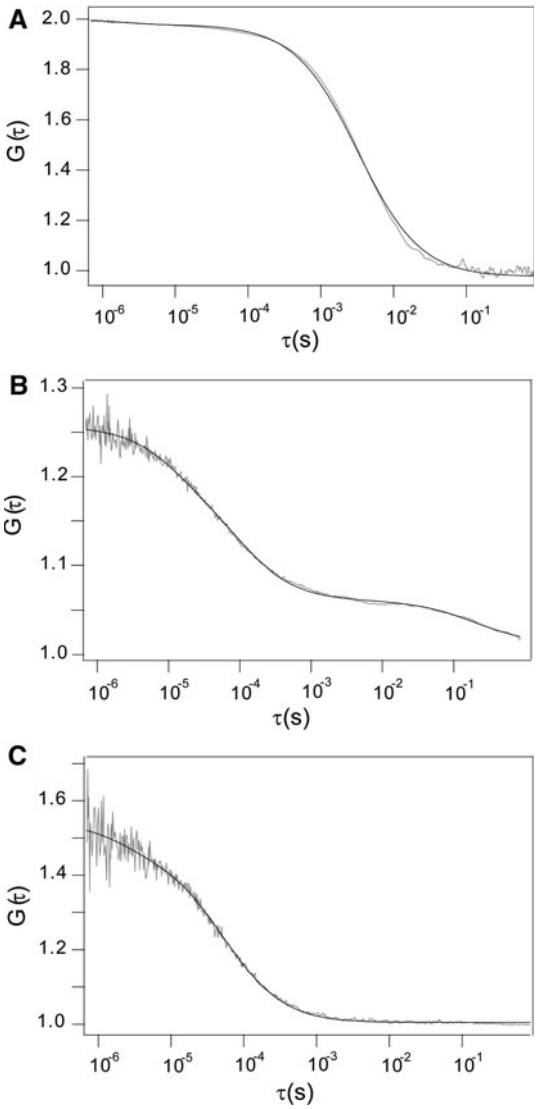

Fig. 3 The action of Y2 on Rhodamine-entrapping vesicles (REVs). **a** POPG-REVs in the absence of Y2. **b** In the presence of 10 μM Y2 the POPG-REV leak and aggregate. This can be seen at the two distinct decays of the correlation function, one at short times on the time scale expected for free dye, and one at long times with a characteristic time longer than the one seen for POPG-REVs alone. **c** Correlation curve for the dye alone in solution. The light *gray curves* are the raw data and the *black curves* represent fits to one (**a**, **c**) or two **b** particle models. The correlation curve in **b** is essentially a combination of the curves of vesciles in **a** and dye in **c**

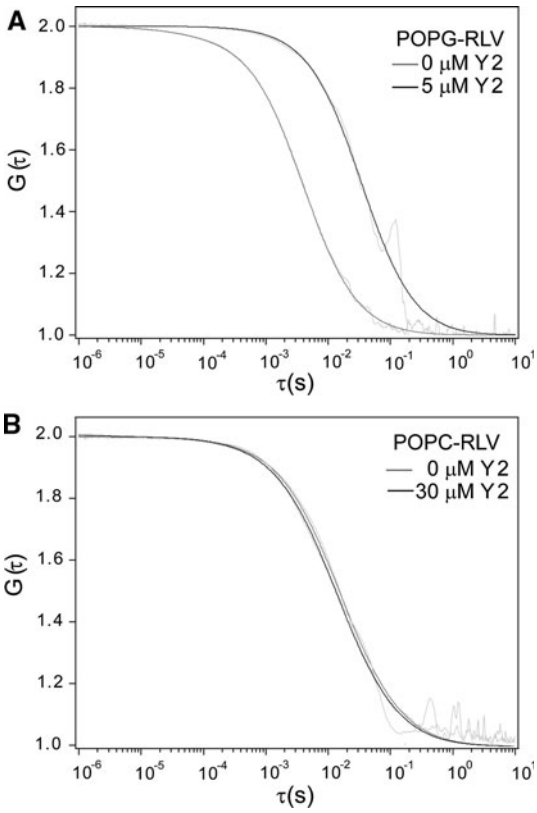

Fig. 4 Example FCS curves showing the interaction of the peptide Y2 with Rhodamine-labeled vesicles (RLVs). All *curves* have been normalized to the same amplitude to allow a better comparison of the width and thus the diffusion times. The diffusion times then give a direct indication of the size of the vesicles. The light *gray curves* are the raw data, the *dark gray* and *black curves* represent fits of diffusion models to the data. **a** POPG-RLVs in the presence and absence of Y2. The width of the curves increases in the presence of Y2, indicating vesicle aggregation. **b** POPC-RLVs in the presence and absence of Y2. Even at concentrations as high as 30 μM no effect of Y2 on the vesicles is detectable

concentration of 5 μM of Y2 observed from antibacterial activity is very close to the concentration range of 5–10 μM for vesicle aggregation of POPG-REV and POPG-RLV observed from FCS. This also fits the transition midpoint of 20 μM of Y2 to form a noncovalent dimer, which was observed by NMR in 30 mM DPC. In our previous study by NMR and molecular dynamic simulations (MD) of selected C-terminal analogues Y2, F2 and C2 (Bai et al. 2009), Y2 showed higher antibacterial activity against the Gram-negative bacteria *P. aeruginosa* and lower cytotoxicity against mammalian cells compared to wt hBD3. The underlying physico-chemical properties distinguishing Y2 and lower activity group peptides (F2, C2 and H2) include the propensity to oligomerize and to accrete unique structures both in water and on the surface of lipid membranes. Molecular dynamics simulations showed a higher stability of the Y2 and F2 dimers compared to C2. This originates mainly from π/π stacking and hydrophobic interactions between the Tyr and Phe aromatic side chains. The prominent structural difference between Y2- and F2-dimers might underline differences in their activity. The Y2-dimer maintains a hairpin like, more compact configuration, in striking contrast to a twisted helical, extended structure of F2-dimer. The compact structure of Y2-dimer induces a higher charge density. In addition, the Tyr residues are involved in aromatic stacking interactions as well as in intra-molecular hydrogen bonds

with surrounding polar groups that, in turn, further stabilizes the compact configuration.

Conclusion

W2, V2, especially Y2, showed higher antibacterial activity selectively against *P. aeruginosa* ATCC 9027 compared to other 10-residue analogues. Covalent V2-dimer showed more potent antibacterial activity than V2-monomer. This series of 10-residue C-terminal analogues and V2-dimer exhibited less toxicity to mammalian cells even at high concentration of up to 200 μg/ml. All these analogues exhibited selective toxicity, towards the negatively charge POPG vesicles in contrast to the zwitterionic POPC vesicles even at relatively high peptide/lipid (P/L) ratio. Our data from FCS, NMR and MD showed stable covalent dimerization, the ability to dimerize and adopt a well-defined structure upon interactions with lipid membranes that contribute to compacting of positive charges within peptide oligomers. The charge density, mediated by corresponding 3D structures, was found to directly correlate with the antimicrobial activity. These novel observations, such as stable covalent dimerization, the ability of noncovalent dimerization, compactness and charge density, may provide a new reasoning on the design of improved antimicrobial peptides.

Acknowledgments This work was supported by the National Medical Research Council of Singapore (NMRC) grants: 1106/2007, 0808/2003, BMRC/R652/73/2008. OLB, LG, and TW were supported by a faculty research council grant from the National University of Singapore (R-143-000-338-112).

References

Bai Y, Liu SP, Jiang P, Zhou L, Li J, Tang C, Verma C, Mu YG, Beuerman RW, Pervushin K (2009) Structure-dependent charge density as a determinant of antimicrobial activity of peptide analogues of defensin. Biochemistry 48:7229–7239

Bauer F, Schweimer K, Kluver E, Conejo-Garcia JR, Forssmann WG, Rosch P, Adermann K, Sticht H (2001) Structure determination of human and murine beta-defensins reveals structural conservation in the absence of significant sequence similarity. Protein Sci 10:2470–2479

Bevins CL, Martin-Porter E, Ganz T (1999) Defensins and innate host defence of the gastrointestinal tract. Gut 45:911–915

Boman HG (1995) Peptide antibiotics and their role in innate immunity. Annu Rev Immunol 13:61–92

Cullor JS, Mannis MJ, Murphy CJ, Smith WL, Selsted ME, Reid TW (1990) In vitro antimicrobial activity of defensins against ocular pathogens. Arch Ophthalmol 108:861–864

Dhople V, Krukemeyer A, Ramamoorthy A (2006) The human beta-defensin-3, an antibacterial peptide with multiple biological functions. Biochim Biophys Acta 1758:1499–1512

Diamond G, Bevins CL (1998) beta-Defensins: endogenous antibiotics of the innate host defense response. Clin Immunol Immunopathol 88:221–225

Diebold Y, Calonge M, Enriquez de Salamanca A, Callejo S, Corrales RM, Saez V, Siemasko KF, Stern ME (2003) Characterization of a spontaneously immortalized cell line (IOBA-NHC) from normal human conjunctiva. Invest Ophthalmol Vis Sci 44:4263–4274

Dunsche A, Açil Y, Dommisch H, Siebert R, Schröder JM, Jepsen S (2002) The novel human beta-defensin-3 is widely expressed in oral tissues. Eur J Oral Sci 110:121–124

Ganz T, Lehrer RI (1995) Defensins. Pharmacol Ther 66:191–205

Hancock RE, Falla T, Brown M (1995) Cationic bactericidal peptides. Adv Microb Physiol 37:135–175

Hopp TP, Woods KR (1981) Prediction of protein antigenic determinants from amino acid sequences. Proc Natl Acad Sci USA 78:3824–3828

Hwang PM, Vogel HJ (1998) Structure–function relationships of antimicrobial peptides. Biochem Cell Biol 76:235–246

Kluver E, Schulz-Maronde S, Scheid S, Meyer B, Forssmann WG, Adermann K (2005) Structure-activity relation of human beta-defensin 3: influence of disulfide bonds and cysteine substitution on antimicrobial activity and cytotoxicity. Biochemistry 44:9804–9816

Kluver E, Adermann K, Schulz A (2006) Synthesis and structure-activity relationship of beta-defensins, multi-functional peptides of the immune system. J Pept Sci 12:243–257

Krouglova T, Vercammen J, Engelborghs Y (2004) Correct diffusion coefficients of proteins in fluorescence correlation spectroscopy. Application to tubulin oligomers induced by Mg2+ and paclitaxel. Biophys J 87(4):2635–2646

Li J, Raghunath M, Tan D, Lareu RR, Chen Z, Beuerman RW (2006) Defensins HNP1 and HBD2 stimulation of wound-associated responses in human conjunctival fibroblasts. Invest Ophthalmol Vis Sci 47:3811–3819

Liu SP, Zhou L, Li J, Suresh A, Verma C, Foo YH, Yap EP, Tan DT, Beuerman RW (2008) Linear analogues of human beta-defensin 3: concepts for design of antimicrobial peptides with reduced cytotoxicity to mammalian cells. ChemBioChem 9:964–973

Magde D, Webb WW, Elson EL (1972) Thermodynamic fluctuations in a reacting system: measurement by fluorescence correlation spectroscopy. Phys Rev Lett 29:705–708

McDermott AM, Redfern RL, Zhang B, Pei Y, Huang L, Proske RJ (2003) Defensin expression by the cornea: multiple signalling pathways mediate IL-1beta stimulation of hBD-2 expression by human corneal epithelial cells. Invest Ophthalmol Vis Sci 44:1859–1865

Parks QM, Hobden JA (2005) Polyphosphate kinase 1 and the ocular virulence of *Pseudomonas aeruginosa*. Invest Ophthalmol Vis Sci 46:248–251

Persson D, Thorén PE, Nordén B (2001) Penetratin-induced aggregation and subsequent dissociation of negatively charged phospholipid vesicles. FEBS Lett 505:307–312

Pramanik A, Thyberg P, Rigler R (2000) Molecular interactions of peptides with phospholipid vesicle membranes as studied by fluorescence correlation spectroscopy. Chem Phys Lipids 104:35–47

Raguse TL, Porter EA, Weisblum B, Gellman SH (2002) Structure–activity studies of 14-helical antimicrobial beta-peptides: probing the relationship between conformational stability and antimicrobial potency. J Am Chem Soc 124:12774–12785

Raj PA, Dentino AR (2002) Current status of defensins and their role in innate and adaptive immunity. FEMS Microbiol Lett 206:9–18

Schmitt MA, Weisblum B, Gellman SH (2007) Interplay among folding, sequence, and lipophilicity in the antibacterial and hemolytic activities of alpha/beta-peptides. J Am Chem Soc 129:417–428

Yeaman MR, Yount NY (2003) Mechanisms of antimicrobial peptide action and resistance. Pharmacol Rev 55:27–55

Yu LL, Ding JL, Ho B, Wohland T (2005) Investigation of a novel artificial antimicrobial peptide by fluorescence correlation spectroscopy: An amphiphilic cationic pattern is sufficient for selective binding to bacteria type membranes and antimicrobial activity. Biochem Biophys Acta 1716:29–39

Yu L, Tan M, Ho B, Ding JL, Wohland T (2006) Determination of critical micelle concentrations and aggregation numbers by fluorescence correlation spectroscopy: aggregation of a lipopolysaccharide. Anal Chim Acta 556:216–225

Yu L, Ding JL, Ho B, Feng SS, Wohland T (2008) Investigation of the mechanisms of antimicrobial peptides interacting with membranes by fluorescence correlation spectroscopy. Open Chem Phys J 1:62–80

Zhou L, Huang LQ, Beuerman RW, Grigg ME, Li SF, Chew FT, Ang L, Stern ME, Tan D (2004) Proteomic analysis of human tears: defensin expression after ocular surface surgery. J Proteome Res 3:410–416